

Integrative and conjugative elements associated with antimicrobial resistance in multidrug resistant *Pasteurella multocida* isolates from bovine respiratory disease (BRD)-affected animals in Spanish feedlots

Carlos Serna^a, Johan Manuel Calderón Bernal^a, Laura Torre-Fuentes^b, Ángel García Muñoz^c, Alberto Díez Guerrier^{a,b}, Marta Hernández^d, José Francisco Fernández-Garayzábal^{a,b}, Ana Isabel Vela^{a,b}, Dolores Cid^a and Julio Alvarez^{a,b}

^aDepartamento de Sanidad Animal, Facultad de Veterinaria, Universidad Complutense, Madrid, Spain; ^bCentro de Vigilancia Sanitaria Veterinaria (VISAVET), Universidad Complutense, Madrid, Spain; ^cDepartamento de Producción y Sanidad Animal, Salud Pública Veterinaria y Ciencia y Tecnología de los Alimentos, Facultad de Veterinaria, Universidad Cardenal Herrera-CEU, CEU Universities, Valencia, Spain; ^dLaboratorio de Biología Molecular y Microbiología, Instituto Tecnológico Agrario de Castilla y León, Valladolid, Spain

ABSTRACT

The emergence of multidrug-resistance (MDR) in *Pasteurella multocida*, a major contributor to bovine respiratory disease (BRD) is being increasingly reported, often linked to the carriage of antimicrobial resistance genes (ARGs) on integrative and conjugative elements (ICEs). The resistance phenotype for 19 antimicrobials was determined using broth microdilution in 75 *Pasteurella multocida* isolates from healthy and BRD-affected cattle from five feedlots. The genomes of 32 isolates were sequenced to identify ARG and mobile genetic elements (MGEs) and assess their genetic diversity. MDR isolates (with phenotypic resistance to aminoglycosides, macrolides, fluoroquinolones and/or tetracyclines) were primarily found among BRD-affected compared to healthy animals. Non-susceptible isolates, belonging to ST79 and ST13, harbored point mutations and four to nine ARGs, including rarely reported mechanisms in Europe (*mph*(E), *msr*(E) and *aadA31* ARGs and newly described mutations in the *gyrA*/*parC* genes). All ARGs were linked to the presence of MGEs including two ICEs, Tn7407 and the novel Tn7809, a prophage and a putative composite transposon. Clonally related isolates were found in different batches from the same feedlot, suggesting maintenance of MDR strains. Our findings demonstrate the diverse genetic basis of AMR in *P. multocida* from BRD-affected cattle in Spain, emphasizing the role of MGEs in the ARG dissemination.

ARTICLE HISTORY

Received 24 September 2024
Accepted 24 February 2025

KEYWORDS



Pasteurella multocida;
bovine respiratory
disease; genotyping;
antimicrobial resistance;
multidrug-resistance;
mobile genetic elements;
integrative conjugative
elements


1. Introduction

Bovine respiratory disease (BRD) is the most significant health and economic problem in intensive beef production systems (i.e. feedlots) worldwide, due to high morbidity, mortality, loss of weight gain and treatment costs (Smith et al. 2020; Snyder and Credille 2020). Multiple viral infections and environmental and management factors, primarily those that overwhelm the host defenses, can lead to an overgrowth of BRD bacterial pathogens in the lower respiratory tract of individual animals, favoring the occurrence of clinical disease (Snyder and Credille 2020). Stress generated by weaning, transport to feedlots, as well as commingling constitute well-known risk factors for BRD, which occurs mainly in

the first weeks after arrival to the feedlot (Chen et al. 2022; Maples et al. 2022). When animals are diagnosed with BRD antimicrobials can be used both as part of individual treatments and as a group metaphylactic treatment to reduce the morbidity and mortality of BRD in high-risk cattle, mainly at the entry to feedlots (Maples et al. 2022; Crosby et al. 2023). Therefore, BRD is the main cause of antimicrobial use (AMU) in cattle feedlots.

AMU in feedlots drives antimicrobial resistance (AMR) selection in BRD-associated pathogens, and increases the risk of transforming opportunistic pathogenic bacteria present in the respiratory tract of the animals into reservoirs of multidrug resistance (Catry et al. 2016; Andrés-Lasheras et al. 2022; Becker et al. 2022). The isolation of multidrug-resistant

CONTACT Dolores Cid  lcid@ucm.es  Departamento de Sanidad Animal, Facultad de Veterinaria, Universidad Complutense, Av. Puerta de Hierro s/n, Madrid 28040, Spain

 Supplemental data for this article can be accessed online at <https://doi.org/10.1080/01652176.2025.2474220>.

© 2025 The Author(s). Published by Informa UK Limited, trading as Taylor & Francis Group.

This is an Open Access article distributed under the terms of the Creative Commons Attribution-NonCommercial License (<http://creativecommons.org/licenses/by-nc/4.0/>), which permits unrestricted non-commercial use, distribution, and reproduction in any medium, provided the original work is properly cited. The terms on which this article has been published allow the posting of the Accepted Manuscript in a repository by the author(s) or with their consent.

(MDR) strains, defined as those resistant to three or more antimicrobial families, and extensively drug-resistant (XDR) strains, those non-susceptible to at least one agent in all but two or fewer antimicrobial classes, has lately become a more frequent occurrence in BRD bacterial pathogens, including *Pasteurella multocida*, a commensal resident of the bovine respiratory tract and one of the main bacterial pathogens involved in BRD (Klima et al. 2020; Calderón Bernal et al. 2023; Jobman et al. 2023). An increase in resistance of BRD bacterial pathogens isolated from cattle after several days or weeks in feedlots compared to those isolated from animals at their arrival has been reported (Woolums et al. 2018; Guo et al. 2020; Hirsch et al. 2022; Calderón Bernal et al. 2023). Moreover, the use of parental macrolides such as tulathromycin in metaphylactic treatments at arrival in the feedlot has been linked to increased MIC against macrolides in BRD Pasteurellaceae (Nobrega et al. 2021) and to increased risk of isolation of MDR strains (Crosby et al. 2023).

MDR in BRD-Pasteurellaceae pathogens is mainly associated with integrative and conjugative elements (ICEs) containing antimicrobial resistance genes (ARGs) conferring resistance to multiple antimicrobial classes. ICEs are self-transmissible elements integrated into the bacterial host chromosome that can excise themselves and be exchanged horizontally between bacteria of the family Pasteurellaceae and other Gram-negative bacteria (Michael et al. 2018). These elements likely play a key role in the concentration and dissemination of ARGs in BRD pathogens (Michael et al. 2018; Snyder and Credille 2020; Andrés-Lasheras et al. 2022). The widespread distribution of ICEs that carry multiple ARGs (MDR-ICEs) is concerning because of their potential role in the dissemination of MDR in a single genetic transfer event (Snyder and Credille 2020; Andrés-Lasheras et al. 2022). The first MDR-ICE described in Pasteurellaceae was ICEPmu1 in *P. multocida* (Michael et al. 2012b). This ICE confers resistance to up to twelve antimicrobials including tetracyclines, florfenicol, sulphonamides, spectinomycin, enrofloxacin, tilmicosin, and tulathromycin. Since then, the presence of ICEs with similar backbone regions associated with MDR in Pasteurellaceae has been documented in several studies in North American feedlots (Klima et al. 2014, 2016; Stanford et al. 2020), but data on the genetic basis of AMR in BRD-bacterial pathogens in Europe are scarce and based on a very limited number of isolates (Schink et al. 2022; Calderón Bernal et al. 2023).

The main aim of this study was to characterize the genetic mechanisms and genetic diversity present in a collection of *P. multocida* isolates with different antimicrobial resistance profiles from both apparently healthy and BRD-affected animals during the fattening period, with a focus on the presence of ICEs associated with antimicrobial resistance mechanisms. Additionally, the persistence of specific resistant clones over multiple batches in selected feedlots was evaluated over time.

2. Material and methods

2.1. Bacterial strains

A total of 75 *P. multocida* isolates coming from apparently healthy beef calves sampled at the entry to the feedlot ($n=50$) and from calves affected by BRD during the fattening period ($n=25$) and belonging to 15 different animal batches housed in one of five feedlots located in two different regions of Spain (Madrid and Valencia) were included in this study (Supplementary Table S1). Sixty out of 75 isolates were recovered from 11 batches in feedlot 1 and 15 isolates were recovered from four batches in feedlots 2 to 5 (Supplementary Table S1). Isolates were obtained in a previous study (Calderón Bernal et al. 2023). Briefly, apparently healthy animals in batches of crossbred beef calves (5–7 months old, 5 to 20 animals/batch), entering one of five feedlots from January 2021 to September 2022 were sampled on the second day after arriving at the feedlot. In addition, all animals that developed clinical signs compatible with BRD during the fattening period (6–7 months) in the batches followed-up were also sampled on the first day clinical signs were observed and before antimicrobial treatment. Animals with clinical signs compatible with BRD were defined as those with nasal or ocular discharges, spontaneous cough, difficult breathing, or a rectal temperature of $>40^{\circ}\text{C}$. Samples consisted of deep nasopharyngeal swabs (DNPS Dryswab laryngeal MW128, MWE Medical Wire, Corsham, UK; $n=237$) or bronchoalveolar lavage (BAL; $n=24$). *Pasteurella multocida* strains were isolated on Columbia agar supplemented with 5.0% sheep blood (BioMérieux España, Madrid, Spain) and identified by MALDI-TOF MS (Bruker Daltonik GmbH, Germany) and a species-specific PCR assay targeting the *kmt1* gene as previously described (Calderón Bernal et al. 2022).

2.2. Antimicrobial susceptibility testing (AST)

Minimum inhibitory concentrations (MIC) for 19 antimicrobials (Table 1) were determined using the broth microdilution method as described in the Clinical and Laboratory Standards Institute Guidelines (Clinical and Laboratory Standards Institute (CLSI), 2008) in commercially available Bovine/Porcine plates (Sensititre™ BOPO7F, Thermo Scientific, Madrid, Spain). Sensititre plates were inoculated according to manufacturer's instructions with isolates suspended in Mueller-Hinton Broth supplemented with 3.0% lysed horse blood. Plates were sealed, and incubated at 37°C aerobically for 24 h and, the MIC, defined as the lowest concentration of an antimicrobial agent that completely prevents visible growth of the test strain under the defined *in vitro* conditions, was assigned by eye. MIC50 and MIC90, values above which the growth of 50.0% and 90.0% of the isolates respectively was inhibited, were also determined. Isolates were classified as wild type (WT) or non-wild type (NWT)

Table 1. Distribution of minimum inhibitory concentrations (MICs) among the 75 *P. multocida* isolates from BRD-affected animals during the fattening period ($n=25$) and from apparently healthy animals at the entry to the feedlots ($n=50$).

CLASS	Antimicrobial	Distribution (no. of isolates) of MICs ($\mu\text{g/mL}$)															% of non-WT or non-S isolates from animals		
																	MIC 50% ($\mu\text{g/mL}$)	MIC 90% ($\mu\text{g/mL}$)	Total
		≤ 0.12	0.25	0.5	1	2	4	8	16	32	64	128	256	512	2/38	4/76			
B lactams	AMP ^a	<75	1						>								≤ 0.25	≤ 0.25	0.0
	PEN ^b	<69	6					>									≤ 0.12	≤ 0.12	0.0
	XLN ^b	<69															≤ 0.25	≤ 0.25	0.0
	GEN ^a		5	<16	1	1	19										2	4	0.0
Aminoglycoside	NEO ^a					<46	6			3	12						≤ 4	>32	20.0 ^d
	SPE ^a								39	27	1	8					16	64	10.7 ^d
	TYLT								19	29	18						32	>32	2.0
Macrolide	TIP ^a																≤ 1	4	2.0
	TIL ^a																4	>16	9.3 ^d
	TUL ^a																≤ 1	>8	29.3 ^d
	GAM ^a																≤ 8	>64	28.0 ^d
Fluoroquinolone	ENRO ^b	<63	1	1	7	2	1		21								≤ 0.12	1	14.7 ^d
	DANO ^b	<61	1	2	2	9											≤ 0.12	>1	17.3 ^d
Lincosamides	CLIN																>16	>16	8.0
	FFN ^a																0.5	1	5.3
Phenicol	TET ^a																≤ 0.5	>8	32.0 ^d
Tetracycline	TIA ^{a,c}																16	32	8.0
Pleuromutilin	SDM ^{b,c}																>256	>256	
Sulfonamides	SXT																$\leq 2/38$	>2/38	

AMP, ampicillin; Pen, penicillin; XLN, ceftiofur; GEN, gentamicin; NEO, neomycin; SPE, spectinomycin; TYLT, Tylosin tartrate; TIP, tildipirosin; TIL, tilmicosin; TUL, tulathromycin; GAM, gamithromycin; ENRO, enrofloxacin; DANO, danofloxacin; CLIN, clindamycin; FFN, florfenicol; TET, tetracycline; TIA, tiamulin; SDM, sulfadimethoxine; SXT, trimethoprim-sulfamethoxazole.

In bold numbers of resistant (non-wild type or non-susceptible) isolates according to the cut-off used. The vertical red line shows the break point used.

^aNon-wild type (non-WT) interpretation according to the epidemiological cut-off (EUCAST).

^bNon-susceptible (non-S) interpretation according to CLSI clinical breakpoints (vet15:2023): penicillin (≤ 0.25 ; 0.5 I; ≥ 1 R); ceftiofur (≤ 0.25 ; 4 I; ≥ 8 R); tilmicosin (≤ 8 ; 16 I; ≥ 32 R); danofloxacin (≤ 0.25 ; 0.5 I; ≥ 1 R) and sulfadimethoxine (≤ 64 S; ≥ 256 R).

^cCut-off out of MIC range.

^dDifferences statistically significant ($p < 0.05$).

Shaded cells indicate concentrations outside of the ranges tested.

using the epidemiological cut-offs (ECOFFs) of the European Committee on Antimicrobial Susceptibility Testing (EUCAST) when available, and as susceptible (S) or non-susceptible (intermediate or resistant; NS) based on the clinical breakpoints according to Clinical and Laboratory Standards Institute (CLSI) guidelines otherwise (Table 1). Multidrug resistance was defined as acquired non-susceptibility to at least one agent in three or more antimicrobial classes. The association between antimicrobial susceptibility and clinical origin of the isolates was determined using the Fisher exact test with the Benjamini-Hochberg adjustment for multiple comparisons using $p < 0.05$ as the threshold for statistical significance in R (R Core Team 2021).

2.3. Whole genome sequencing (WGS), quality check and genome assembly and annotation

Whole genome sequences of a subset of 32 *P. multocida* isolates that included all resistance profiles present in the collection (Table 2) were analyzed; this selection comprised 18 isolates sequenced for this study in an Illumina platform (seven from healthy and eleven from clinically affected animals) and 14 isolates (eight from healthy and six from clinically affected animals) previously sequenced (Calderón Bernal et al. 2023). Briefly, DNA was extracted and purified using the Qiagen DNA Blood & Tissue Kit, followed by quantification with a Qubit® fluorometer (Invitrogen; Waltham, MA, USA). Library preparation for these samples was performed using the Nextera XT DNA Library Preparation Kit according to standard protocols (Illumina, Inc., San Diego, CA). Sequencing was performed on the MiSeq Illumina platform, using V3 reagents with 2×300 cycles. In addition, eight of those isolates subjected to Illumina sequencing that contained ARGs potentially linked to ICEs (see Section 3) were selected for long-read sequencing on a MinION Nanopore device (Oxford Nanopore Technologies, UK).

Raw Illumina reads were initially trimmed using Trimmomatic (Bolger et al. 2014) and quality was assessed with FastQC (Andrews 2010). Short reads from all 32 isolates passed the quality control checks and were assembled using SPAdes (Bankevich et al. 2012). In addition, hybrid genome assembly using short and long reads for isolates subjected to MinION sequencing was carried out using the FullForcePlasmidAssembler (FFPA) pipeline (<https://github.com/MBHallgren/FullForcePlasmidAssembler>). FFPA uses Qcat (<https://github.com/nanoporetech/qcat/tree/master/qcat>) for the removal of adapter and barcode sequences and NanoFilt (De Coster et al. 2018) for the removal of low-quality reads. Hybrid assembly was performed by Unicycler (Wick et al. 2017) and the assembly graphs were visualized with Bandage (Wick et al. 2015). Quast (Gurevich et al. 2013) was used to evaluate the quality of assemblies. Both short-read and hybrid assemblies were annotated with Bakta v1.8.2 (Schwengers et al. 2021) (Supplementary Table S2).

Table 2. Resistance patterns among 75 *P. multocida* isolates belonging to BRD-affected animals ($n=25$) and apparently healthy animals ($n=50$) at the entry to feedlots (only antimicrobials in which at least one non-wild type or non-sensible isolates was found are included).

Resistance pattern ^a	Number of antimicrobial families with resistance	Aminoglycosides		Macrolides			Fluoroquinolones		Phenicolos	Tetracyclines		<i>P. multocida</i> isolates		Animal source	No. of WGS
		NEO	SPE	TIP	TUL	GAM	ENRO	DANO	FFN	TET	MDR	n	%		
1	4										Yes	4	5.3	BRD/healthyb	4
2	4										Yes	3	4.0	BRD	2
3	3										Yes	4	5.3	BRD/healthyb	3
4	4										Yes	6	8.0	BRD	4
5	3										Yes	4	5.3	BRD	3
6	3										Yes	1	1.3	BRD	1
7	2										No	1	1.3	healthy	1
8	2										No	1	1.3	healthy	1
9	1										No	1	1.3	healthy	1
10	0										No	50	66.6	BRD/healthyb	12

MDR, multiresistant. / NEO, neomycin; SPE, spectinomycin; TIP, tildipirosin; TUL, tulathromycin; GAM, gamithromycin; ENRO, enrofloxacin; DANO, danofloxacin; FFN, florfenicol; TET, tetracycline; /BRD, Bovine respiratory disease.

^aAll the isolates were susceptible to PEN, XNL and wild type for AMP and GEN.

^bThree, three and five isolates in resistance patterns 1, 3 and 10, respectively, were from BRD-affected animals with the remaining isolates originating from healthy animals.

2.4. *In silico* genotyping: MLST, antimicrobial resistance genes and mobile genetic elements (MGEs)

In silico multi-locus sequence typing (MLST) was performed against the RIRDC MLST scheme using the MLST software (<https://github.com/tseemann/mlst>). Detection of known antimicrobial resistance genes was conducted using AMRFinder v3.12.8 (database version 2024-01-31.1) (Feldgarden et al. 2021) with an identity threshold of >80.0%. For the identification of point mutations associated with resistance, known single nucleotide polymorphisms (SNPs) in the 23S rRNA (linked to macrolide resistance), *rpsE* (spectinomycin resistance), and *gyrA* and *parC* (both associated with quinolone resistance) genes (Kehrenberg and Schwarz 2007; Kong et al. 2014; Olsen et al. 2015) were identified through the alignment of short reads to the *P. multocida* strain FDAARGOS_218 reference genome (CP020405.2) using Snippy (<https://github.com/tseemann/snippy>). The presence of plasmid replicons in the *P. multocida* isolates was assessed using PlasmidFinder (Carattoli et al. 2014) with an identity threshold of >80.0% and MOB-suite (Robertson and Nash 2018) with default parameters.

To detect accessory regions on the chromosome linked to mobile genetic elements, we used the annotated hybrid assemblies for whole genome alignment with Progressive MAUVE v2015_02_25 (Darling et al. 2004). In these regions, the presence of conjugation apparatus indicative of integrative and conjugative elements (ICEs) was investigated using MacSyFinder v2.0, employing the CONJScan v2.0.1 models (Cury et al. 2020; Néron et al. 2023). The presence of prophage structural genes was also evaluated with PHASTEST v3.0 (Wishart et al. 2023). Short-read assemblies were then scrutinized for characterized MGEs using NUCmer v3.146 (Marçais et al. 2018), applying stringent selection criteria (alignment of ≥98.0% of their length and an identity of ≥98.0% with complete ICEs or prophages) to confirm matches.

2.5. Phylogenetic analysis

The phylogenetic relationship between the 32 *P. multocida* isolates from Spanish feedlots analyzed here and seven external *P. multocida* strains from previous studies (Becker et al. 2022; Schink et al. 2022) and included in the National Center for Biotechnology Information (NCBI) Pathogen Detection database was assessed using a SNP-based approach. Assemblies from short reads and hybrid assemblies were aligned with Snippy (<https://github.com/tseemann/snippy>) against the complete sequence of one of the isolates from this study (735CV), used as the reference genome. The multiple alignment obtained from Snippy was used to filter out potential recombinant regions using Gubbins v. 3.1.4 (Croucher et al. 2015) and the number of SNPs identified was extracted with snp-sites v. 2.5.1 (Page et al. 2016). A

maximum-likelihood phylogenetic tree was generated with RAxML v. 8.2.12 (Stamatakis 2014) using the general time-reversible substitution evolutionary model with gamma correction and 1000 bootstrap replicates. The tree was rooted using two sequences from *P. multocida* ST50 (GCA_023555675.1) and *P. multocida* ST122 (GCA_029650805.1) as outgroups. The 'RhierBAPS' package (Tonkin-Hill et al. 2018, 2019) in R (R Core Team 2021) was used to identify clusters in the population through the hierBAPS (hierarchical Bayesian Analysis of Population Structure) algorithm (Corander et al. 2003, 2004; Corander and Marttinen 2006; Cheng et al. 2013) and the tree was visualized with the iTOL editor (Letunic and Bork 2019).

Distances ≤20 SNPs between isolates were considered indicative of a clonal status (Alhamami et al. 2023), and therefore this threshold was applied when investigating the likely persistence of MDR clones across different batches.

3. Results

3.1. Antimicrobial resistance phenotypes of *P. multocida* from BRD-affected and apparently healthy animals

The distributions of the MICs for *P. multocida* isolates are shown in Table 1. Considering antimicrobials for which epidemiological cut-offs were available and within the ranges of concentrations tested (10 out of 19), the proportion of isolates with a NWT phenotype, which was considered suggestive of carriage of acquired resistance mechanisms, ranged from 28.0–32.0% (tulathromycin and gamithromycin and tetracycline) to 10.0–20.0% (spectinomycin and neomycin) or less than 10.0% (tildipirosin and florfenicol), while only isolates with a wild-type phenotype for gentamicin and ampicillin were found (Table 1). For the four antimicrobials in which only clinical cut-offs were available, the proportion of non-susceptible isolates was 14.0–17.0% (enrofloxacin and danofloxacin) or 0% (penicillin and ceftiofur). For the remaining five antimicrobials with no cut-offs available (tylosin tartrate, clindamycin and trimethoprim-sulfamethoxazole) or with cut-offs outside of the range tested (tiamulin and sulfamethoxazole), very high MICs were recorded for all but trimethoprim-sulfamethoxazole, with MIC₉₀ values above the highest concentration tested for all four (Table 1). Resistance levels were significantly ($p < 0.05$) higher in *P. multocida* isolates from BRD-affected animals than in those from apparently healthy animals for all antimicrobials in which a threshold was available and NWT/non-susceptible isolates were detected except for florfenicol (Table 1).

Twenty-five of the 75 *P. multocida* isolates (33.3%) had a NWT/non-susceptible phenotype for at least one antimicrobial (Table 2) with a significantly higher ($p < 0.05$) proportion of resistance among those from BRD-affected animals (20/25; 80.0%) compared with those from apparently healthy calves (5/50; 12.0%). Twenty-two of the 75 isolates (29.3%) had MDR phenotypes (Table 2), the majority of which (13/22)

included resistance to aminoglycosides, macrolides and tetracyclines (Table 2).

3.2. Detection of AMR mechanisms and correlation between resistance genotypes and phenotypes in sequenced *P. multocida* isolates

Out of the 32 sequenced *P. multocida* isolates selected to include all observed resistance patterns, no AMR determinants were found among the 12 isolates with no phenotypic resistance (pattern 10) and in the isolate with a NWT phenotype only for spectinomycin (pattern 9) (Table 2). The remaining isolates ($n=19$) harbored between four and nine ARGs linked to resistance across five antibiotic families: aminoglycosides (*aadA31*, *aph(3'')-Ib*, *aph(3')-Ia* and *aph(6)-Id*), phenicols (*catA3* and *floR*), macrolides (*mefC*, *mphE*, *mphG* and *msrE*), sulphonamides (*sul2*) and tetracyclines (*tet(B)*, *tet(H)* and *tet(Y)*) (Supplementary Table S3). Additionally, mutations in the quinolone resistance-determining regions (QRDR) of the *parC* and *gyrA* genes, as well as a mutation in the 23S rRNA (A2059G) were identified in between one and seven isolates (Supplementary Table S3). None of the five isolates carrying the mutation in the 23S rRNA carried other macrolide-associated ARGs.

The presence of AMR determinants was linked to increased MICs for almost all antimicrobial tested in this study (Figure 1). When the *aph(3')-Ia* gene was found (always in combination with two or three other aminoglycoside ARGs) very high MICs ($>32\mu\text{g/mL}$) were observed for neomycin, while other aminoglycoside modifying enzyme-encoding genes conferred intermediate MICs ($8\text{--}32\mu\text{g/mL}$), though still mostly above the resistance threshold (Figure 1(A)). Similarly, the *aadA31* gene was linked with resistance to spectinomycin (Figure 1(B)). Among the quinolones, point mutations in the *gyrA* (Ser88Ile, Ser88Arg) and *parC* (Ser84Leu, Glu88Lys) genes were associated with resistance to enrofloxacin and danofloxacin, especially when mutations occurred in both genes (Figure 1(C,D)). For macrolides, the resistance phenotype conferred by the AMR mechanisms identified here depended on the antimicrobial: the 23S rRNA mutation A2059G was the only mechanism conferring resistance to tildipirosin (Figure 1E) and was also associated with higher MICs in tilmicosin ($>16\mu\text{g/mL}$), tulathromycin ($>64\mu\text{g/mL}$), and gamithromycin ($>8\mu\text{g/mL}$) compared to isolates harboring other macrolide acquired resistance genes (Figure 1(F–H)). For phenicols and tetracycline-associated ARGs, their presence alone or in combination (tetracycline ARGs) was always linked to resistant phenotypes and very high ($>8\mu\text{g/mL}$) MICs (Figure 1(I,J)). The presence of *sul2* was associated with MICs $>256\mu\text{g/mL}$ to sulfadimethoxine (a single concentration was tested for this antimicrobial) (Figure 1(K)), while no apparent association between the carriage of *sul2* and the MIC to trimethoprim-sulfamethoxazole was found (Figure 1(L)).

3.3. Characterization of mobile genetic elements

Overall, eight of the 32 sequenced isolates exhibited ICEs, with seven of these co-harboring two distinct ICEs on their chromosomes. Three of them contained the previously characterized ICE Tn7407 (Schink et al. 2022), which carried six ARGs, and was found in isolates with a NWT phenotype for tetracycline and neomycin (Table 3). Additionally, five isolates carried a highly similar ICE (99.0% identity with Tn7407, referred to as ICE Tn7407_like) that also included the *aadA31* gene linked to resistance to aminoglycosides (Figure 2(A)). Both the ICE Tn7407 and its variant ICE Tn7407_like were flanked by 8bp direct repeats (5'-ATTCAAAA-3') and were located upstream of the gene encoding the magnesium/cobalt transporter CorC, as previously reported (Schink et al. 2022).

All three isolates carrying the Tn7407 and four of the five with Tn7407_like also carried a 53,350bp-long novel ICE, named ICE Tn7809. This element was flanked by 9bp direct repeats (5'-GATTTTGAA-3') and was integrated in a genomic copy of a tRNA^{Leu}. Tn7809 was highly similar to ICEs Tn7407 and Tn7407_like (95.9% identity) and its conjugation machinery also contained a mating pair formation (MPF) type G system. This ICE harbored a unique resistance region including *sul2*, *mefC*, *mphG*, *aph(6)-Id*, *aph(3'')-Ib*, and *tet(Y)* genes (Figure 2(B)) that was linked to phenotypic resistance to macrolides such as tulathromycin and gamithromycin, which was not observed in the one isolate carrying only the ICE Tn7407_like (1094CM).

In addition, eleven isolates without ICEs carried a prophage containing the *sul2*, *catA3*, *aph(3'')-Ib*, and *tet(B)* genes (Figure 2(C)). Four of these isolates also contained an element flanked by two identical copies of ISMha6, suggesting the existence of a composite transposon. This transposon included multiple copies of ARGs such as *sul2*, *catA3*, *msrE*, *mphE*, *mefC*, *mphG*, *tet(Y)*, *aph(3'')-Ib*, and *aph(6)-Id*, along with five copies of *floR* (Figure 2(D)). This element was found in isolates with a NWT phenotype for florfenicol, tulathromycin, and gamithromycin. Table 3 provides a summary of the findings on the distribution of MGEs, ARGs and phenotypes across the isolates used in this study.

3.4. Genetic diversity in relation to the carriage of ICEs linked to ARGs

The 32 genomes obtained in this study were classified as MLST sequence type ST13 ($n=12$), ST79 ($n=16$) and ST80 ($n=4$). The phylogenetic analysis, including the seven external isolates from previous studies (Becker et al. 2022; Schink et al. 2022), showed three major clades (1–3) separated by 517–1,685 SNPs (Figure 3). Isolates included in the first two clades (1 and 2, containing ST80 and most ST13 isolates, respectively) originated mostly from healthy animals, lacked antimicrobial resistance genes and differed by 1,299–1,559 SNPs between clades (with a within-clade variability of <104 and <302 SNPs for clades 1 and 2).

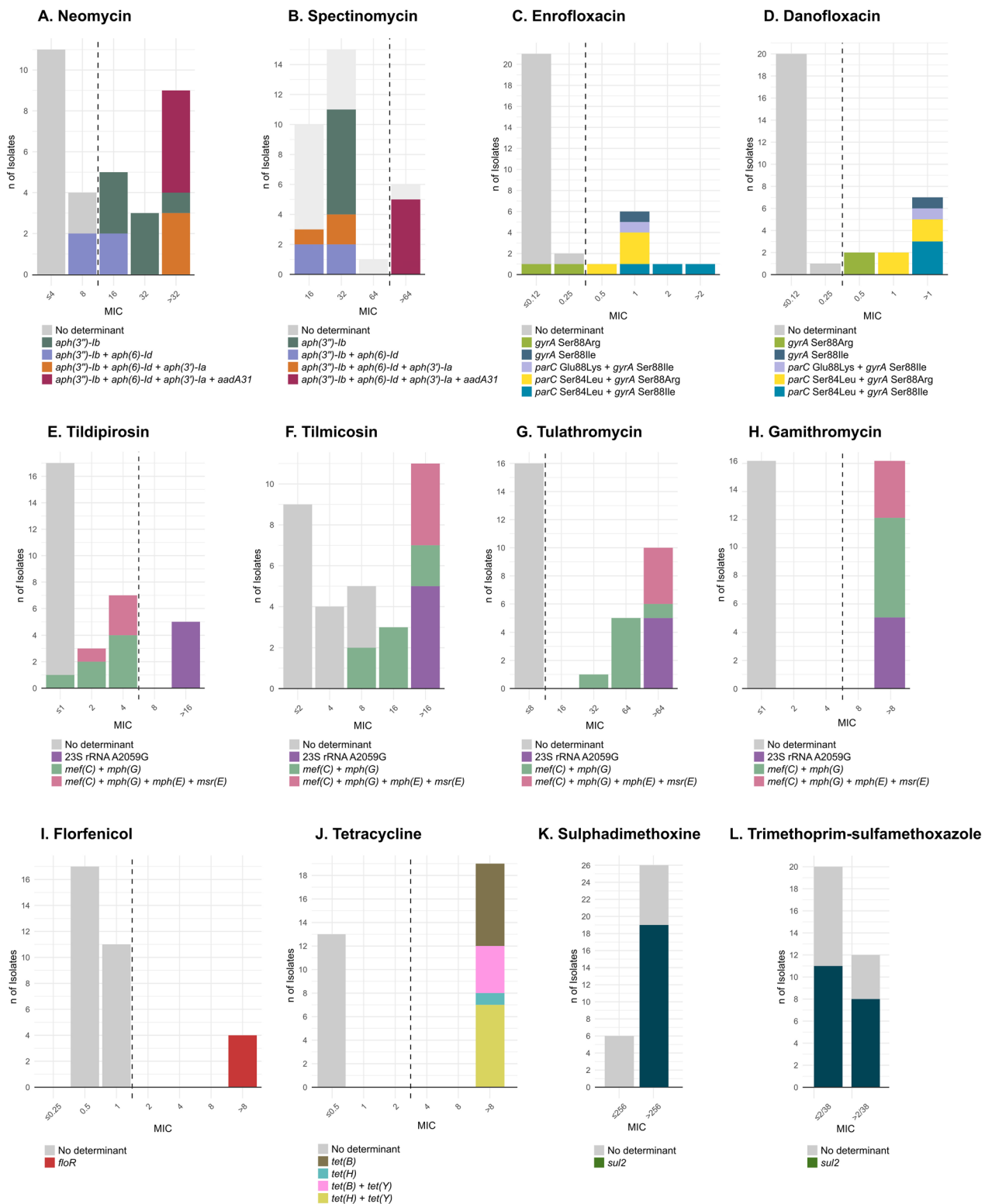


Figure 1. MIC distributions for 32 sequenced *P. multocida* isolates. The bar plots represent the number of isolates exhibiting different minimum inhibitory concentrations (MICs) for each tested antibiotic. Panels (A–L) display individual antibiotics. The distribution of resistance determinants within each bar is shown in different colors. Vertical dotted lines denote the MIC breakpoints used in this study (Table 1).

The third major clade included two different subclades, 3.1 and 3.2, separated by <610 SNPs and both mainly containing strains obtained from clinical animals. Isolates in both subclades harbored a high number of ARGs but carried different MGEs. Subclade 3.1 included 11 strains belonging to ST79 ($n=8$) and ST13 ($n=3$) separated by <205 SNPs that carried all the different chromosomal mutations associated with resistance detected in the study (Figure 3). The three ST13

isolates from this subclade harbored the prophage carrying the *sul2*, *catA3*, *aph(3'')-Ib*, and *tet(B)* resistance genes (Figure 2(C)) and the same three mutations in the QRDR regions. The remaining isolates in this subclade (8/11) belonged to ST79 and in addition to the same prophage four of them also harbored the composite transposon linked to macrolide and florfenicol resistance genes (Figure 2(D)). Subclade 3.2 included eight ST79 strains from this study and seven

ST79 external isolates from the USA, Switzerland and Germany (Figure 3). Except for one external isolate lacking ARGs, the rest of the isolates in this subclade (separated by <64 SNPs, <53 SNPs if only isolates from Spain are considered) carried the highest number of aminoglycoside resistance genes, located either in one ICE (ICE Tn7407 or ICE Tn7407_like) or two ICEs (ICE Tn7407 or ICE Tn7407_like plus ICE Tn7809).

3.5. Persistence of MDR *P. multocida* isolates across multiple batches from the same feedlot

Evidence of a possible clonal relationship (<20 SNPs difference) was observed for seven isolates from subclade 3.2 and for four isolates from subclade 3.1 retrieved from different batches in feedlot 1 (Figure 4(A)). Isolates from subclade 3.2 were retrieved from

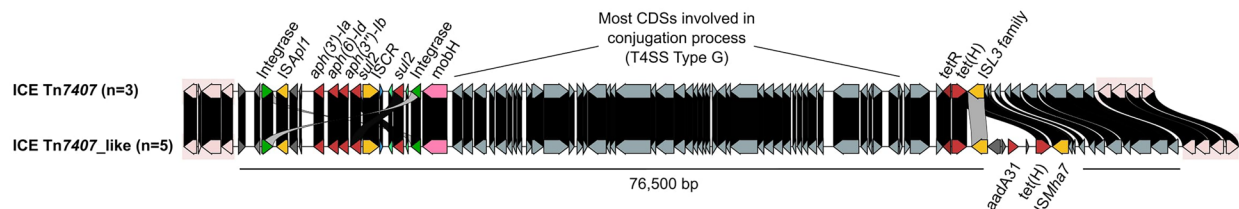
BRD-affected animals in four different batches (LV1, LV4, LV8 and LV9) with entry dates spanning from 13 April 2021 to 18 February 2022 which coexisted in the feedlot for several weeks (Figure 4(B)), with isolates from animals in batches LV1, LV4 and LV9 separated by only 0–6 SNPs. Clonally related isolates in subclade 3.1 were retrieved from three BRD-affected animals and one apparently healthy animal located in two different batches (LV7 and LV5) which were also present simultaneously in the feedlot for several weeks (Figure 4(B)). In addition, three pairs of clonally related isolates retrieved from single batches in feedlot 1 were also found [two of them involving pairs of isolates from apparently healthy animals from clade 1 and subclade 3.1 (104PV-105PV and 282PV-283PV) and the last one involving two isolates from BRD-affected animals from subclade 3.1 (779CV-798CV)] (Figure 4(A)). Finally, two isolates

Table 3. Mobile genetic elements (MGE) detected among the 32 sequenced isolates along with the antimicrobial resistance genes (ARGs) detected within them and associated resistance phenotypes for antimicrobials with available breakpoints.

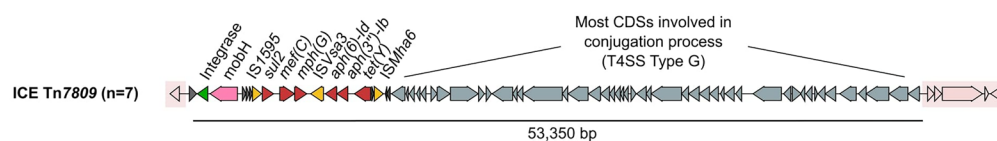
Mobile genetic element (MGE)	No. of isolates (%)	Antimicrobial resistance genes (ARGs)	Resistance phenotype
ICE Tn7407	3 (9.4)	<i>aph(3'')-Ia</i> , <i>aph(6)-Id</i> , <i>aph(3'')-Ib</i> , <i>sul2</i> (x2), <i>tet(H)</i>	NEO-TET
ICE Tn7407_like	5 (15.6)	<i>aph(3'')-Ia</i> , <i>aph(6)-Id</i> , <i>aph(3'')-Ib</i> , <i>sul2</i> (x2), <i>tet(H)</i> (x2), <i>aadA31</i>	NEO-SPE-TET
ICE Tn7809	7 (21.9)	<i>sul2</i> , <i>mefC</i> , <i>mphG</i> , <i>aph(6)-Id</i> , <i>aph(3'')-Ib</i> , <i>tet(Y)</i>	TUL-GAM-TET
ISMha6 element	4 (12.5)	<i>sul2</i> (x3), <i>catA3</i> , <i>aph(3'')-Ib</i> (x3), <i>aph(6)-Id</i> (x3), <i>floR</i> (x5), <i>msrE</i> , <i>mphE</i> , <i>mefC</i> , <i>mphG</i> , <i>tet(Y)</i>	TUL-GAM-FFN-TET
Prophage	11 (34.4)	<i>sul2</i> , <i>catA3</i> , <i>aph(3'')-Ib</i> , <i>tet(B)</i>	TET

NEO, neomycin; SPE, spectinomycin; TUL, tulathromycin; GAM, gamithromycin; FFN, florfenicol; TET, tetracycline.

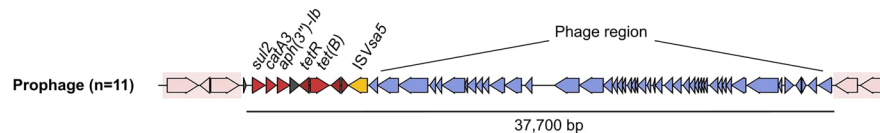
A. ICE Tn7407 and Tn7407_like



B. ICE Tn7809



C. Prophage



D. ISMha6 flanked element

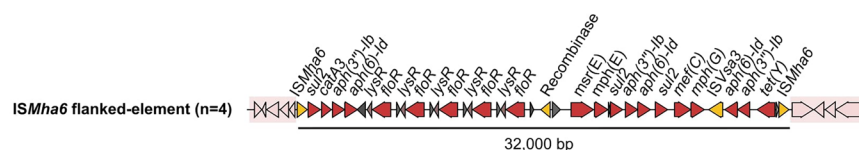


Figure 2. Gene structure of mobile genetic elements identified in this study. Arrows represent open reading frames with the following color codes: integrase in green, insertion sequences (ISs) in yellow, ARGs in red, and relaxase in pink. (A, B) Integrative and conjugative elements (ICEs) Tn7407, Tn7407_like, and the novel ICE Tn7809 identified in this study. The conjugative machinery is indicated by gray arrows. (C) Prophage identified carrying various ARGs. Proteins identified as phage components are colored in purple. (D) Element flanked by two copies of ISMha6, forming a putative transposon containing multiple ARGs and ISs.

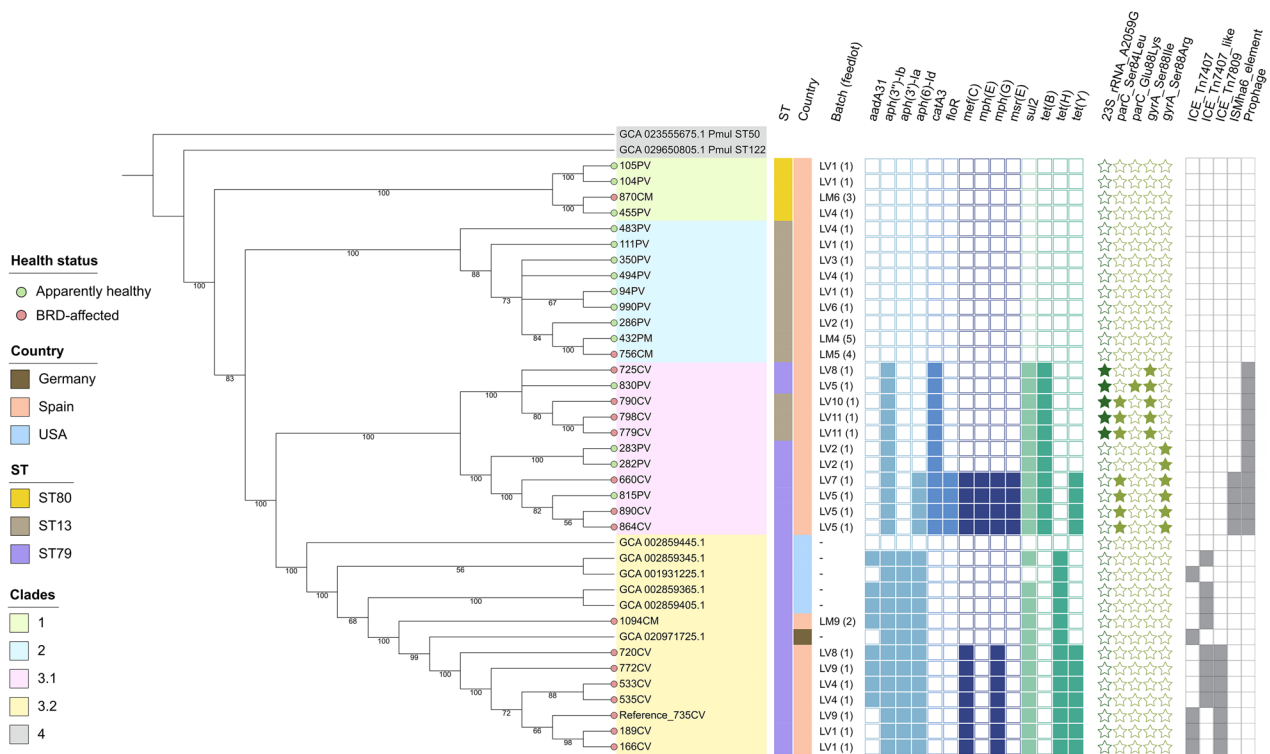


Figure 3. Phylogenetic relationship of *P. multocida* isolates along with carriage of antimicrobial resistance genes (ARGs), point mutations and integrative and conjugative elements (ICE). Dendrogram representation of maximum-likelihood phylogeny based on whole-genome SNPs analysis (branches with bootstrap values >50). The color of the leaves indicates the status of the animal (healthy=green or BRD-affected animals=red).

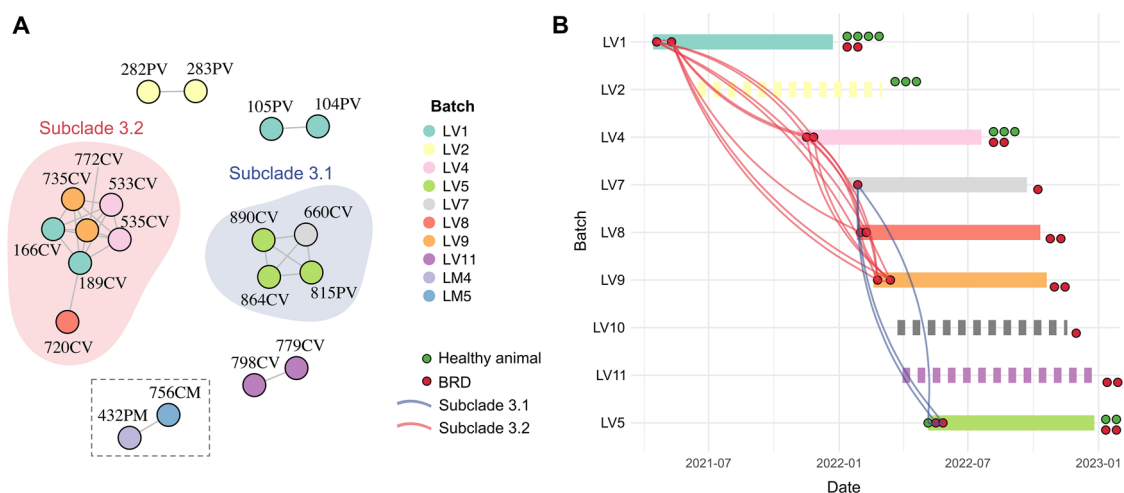


Figure 4. Inferred transmission network based on SNP distance. (A) Each node represents an individual genome, and the edges connecting them indicate a close genetic relationship (less than 20 SNPs). Two main clusters are detected, corresponding to subclades 3.1 and 3.2 of the phylogenetic tree (Figure 3). The nodes are colored according to their respective batches. (B) Entry and exit of the different batches within the feedlot 1. Dots represent individual isolates, and connecting lines show isolates with fewer than 20 SNPs between them, suggesting possible transmission events. The network shows the transmission of two different clones, subclades 3.1 (blue) and 3.2 (red) over time across different batches. To the right of each batch, dots represent the number of sequenced isolates, either from apparently healthy animals (green) or BRD cases (red).

retrieved from a BRD-affected animal and an apparently healthy calf in two batches housed in different feedlots with a 10-month difference (432PM in LM4 and 756 in LM5) were also separated by <20 SNPs.

4. Discussion

The emergence of MDR strains among BRD-bacterial pathogens reduces available options for the effective treatment of the disease and is concerning from a

One Health point of view due to the need to use additional antimicrobials (Anholt et al. 2017; Schönecker et al. 2020; de Jong et al. 2023). For this reason, monitoring of antibiotic resistance in these bacteria is needed (Kudirkiene et al. 2021; Nielsen et al. 2021; de Jong et al. 2023) and is a key step to inform veterinarians on treatment protocol decisions that ensure judicious use of antimicrobials and to design strategies to avoid AMR dissemination (Anholt et al. 2017; de Jong et al. 2023). Even though data

on AMR in BRD associated bacterial pathogens in several countries in Europe is available through scientific studies (Schönecker et al. 2020; Kudirkienė et al. 2021; de Jong et al. 2023) and national AMR monitoring programs including these pathogens (Nielsen et al. 2021; de Jong et al. 2023), limited information on AMR and specifically on the genetic mechanisms behind it in BRD-associated bacterial pathogens in Spain is available, even though it is one of the main beef cattle producers in the European Union (<https://ec.europa.eu/eurostat/>).

A collection of isolates recovered from either clinically affected or healthy calves from different batches in five Spanish feedlots was subjected to phenotypic and genotypic analyses to evaluate the genetic elements associated with clinically relevant resistance phenotypes and if possible assess their persistence over time. Most of the batches (12/15) included in this study, 11 from feedlot 1 and one from feedlot 2, came from five commercial operators (Supplementary Table S1) that commingled purchased animals from multiple origins in a given batch. Since clinically healthy animals were sampled on arrival, they can be considered indicative of the baseline resistance levels in *Pasteurella* before the fattening period. For these animals, the highest levels of resistance among isolates retrieved on arrival involved tetracycline, macrolides and fluoroquinolones, but were all below 10.0% (Table 1). This is in agreement with previous reports describing low levels of AMR in cattle *P. multocida* isolates retrieved at arrival to the feedlots (Guo et al. 2020; Andrés-Lasheras et al. 2021). Differences in the AMR levels among isolates from healthy vs. BRD-affected animals should be interpreted carefully since several clinical isolates originated from batches in isolation of *P. multocida* from healthy animals at feedlot entry was not attempted and *viceversa*, and thus these differences could be due to factors other than the health status of animals, e.g. differences in the populations at arrival or other factors such as management conditions and, most importantly, different antimicrobial usage (Timsit et al. 2017). Despite of this, the level of AMR may vary across countries and may even differ between feedlots because of management factors and, most importantly, different antimicrobial usage (Timsit et al. 2017), and therefore care must be taken when extrapolating this data. Nevertheless, detection of MDR *P. multocida* isolates is worrisome given its potential to rapidly spread as evidenced by the emerging problem in North American feedlots caused by strains with ARGs typically located in ICEs and resistant to multiple antimicrobial families including macrolides, phenicols, aminoglycosides, sulfonamides and tetracyclines (DeDonder and Apley 2015; Alhamami et al. 2023).

Even though the association between the presence of resistance determinants and reduced susceptibility to antimicrobials is not always straightforward in *Pasteurellaceae* (Owen et al. 2017; Beker et al. 2018), here elevated MICs could be linked to the presence of one or more already described resistance mechanisms (ARGs or chromosomal mutations) for

all antimicrobials except for the presence of *sul2* and increased MICs for trimethoprim-sulfamethoxazole and sulfadimethoxine (Figure 1), thus offering proof of their role in the induction of NWT phenotypes. The lack of association between the presence of the *sul2* gene and elevated MICs for sulfonamides was recently reported in *Mannheimia haemolytica* (Kostova et al. 2024) and suggests that additional mechanisms must be involved in reduced susceptibility to this antimicrobial class, though the limited range of concentrations tested here limits our ability to extract definitive conclusions on the role of this gene in the resistance phenotype.

Most of the resistance determinants described here have been previously reported in resistant *P. multocida* strains, though the presence of macrolide resistance genes *mph*(E) and *msr*(E) in European isolates is remarkable since its presence has been reported more commonly in isolates from the United States (Beker et al. 2018) and only very recently in European isolates (Ujvári and Magyar 2022). Furthermore, the *aadA31* aminoglycoside resistance gene, first described in two *P. multocida* isolates retrieved from BRD cases in Canada that carried the gene in a variant of ICE $Mh1$ (Cameron et al. 2018) and whose presence in clinical *P. multocida* isolates from cattle was also recently associated with carriage of ICE $Pmu1$ variants (Stanford et al. 2020), was also found here in four closely related isolates carrying the ICE Tn7407-like, which only differed from Tn7407 in the presence of this gene (Figures 2(A) and 3). Interestingly, four external isolates from samples collected in 2013 in two states of the United States (Supplementary Table S2) also carried this gene in the same ICE (Tn7407-like), demonstrating the widespread distribution of the gene and its circulation in cattle several years before it was first described.

Similarly, resistance to fluoroquinolones is rarely observed in *P. multocida* (Michael et al. 2012a; Melchner et al. 2021; de Jong et al. 2023) but more than one-third of the isolates retrieved from BRD-affected cattle in this study and even few isolates from healthy calves had MICs above the CLSI clinical breakpoints for enrofloxacin and danofloxacin (Table 1), with most resistant isolates (and certainly those with higher MIC values) harboring two mutations resulting in amino acid exchanges in the *gyrA* (codon 88) and *parC* (codon 84 or 88) genes (Figure 1). The location of these mutations, while still within the quinolone resistance-determining regions, is different than those described in the also fluoroquinolone-resistant strain 36950 (which harbored mutations in codons 75 and 83 in *gyrA*) (Michael et al. 2012a) or in other fluoroquinolone-resistant isolates from Japan harboring different mutations (Kong et al. 2014). This therefore highlights the potential for the emergence of new mechanisms leading to resistance to this critically important antimicrobial class in *P. multocida*. In contrast, the chromosomal mutation associated with elevated MICs to all macrolides tested in this study (substitution of adenosine by guanine at position 2059 according to *E. coli* numbering), found in a

subset of isolates in clade 3.1, had been previously described in macrolide-resistant *P. multocida* isolates (Olsen et al. 2015; Beker et al. 2018; Ujvári and Magyar 2022). Another *P. multocida* macrolide-resistant isolate which had been previously sequenced (isolate IMT47951, assembly accession GCA_020971725.1) and carried a mutation in the same location was also included in the phylogeny but fell in a different subclade (3.2) according to our phylogenetic analysis (Figure 3), though in that case the mutation involved a different nucleotide substitution (cytosine instead of guanine here) (Schink et al. 2022).

All the ARGs identified in MDR isolates were linked to the presence of one or more mobile genetic elements in the bacterial genomes (Figure 2). The presence of an ICE containing multiple ARGs (ICE*Pmu1*) was first described in *P. multocida* isolates in North America already a decade ago (Michael et al. 2012b), and homologs of this ICE have since then been found multiple times in isolates from clinically affected cattle in the United States and Canada (Clawson et al. 2016; Klima et al. 2020). However, new ICEs have been recently described in *P. multocida* isolates from Australia (ICE-*PmuST394*) (Roy Chowdhury et al. 2024) and Germany (Tn7407) (Schink et al. 2022), but they are still extremely rare in Europe. Here, in eight phylogenetically related isolates (grouped in subclade 3.2, Figure 3), we found one or two ICEs linked to the presence of between six and nine resistance genes. Seven of these isolates were separated by less than 20 SNPs and were retrieved from clinically affected animals from four batches that were housed in the same feedlot over 18-months (Figure 4). The close genetic proximity between these seven isolates suggests that all are epidemiologically related, suggesting that the same strain could be persisting over time in the feedlot and thus transmission could be taking place at the feedlot. This hypothesis would be supported by the very high similarity (0–6 SNPs) between the six isolates from batches LV1, LV4 and LV9, that entered the feedlot over a 10-month-period.

The seven isolates in subclade 3.2 carried two ICEs, one of which (here named Tn7809) is first described here and has a size (53,350bp) in the range of previously described ICEs in *Pasteurella* (49–79kb) (Beker et al. 2018). The second ICE was either the recently described ICE Tn7407 (Schink et al. 2022), found in three isolates in batches LV1 and LV9, or the Tn7407-like ICE that also contained the *aadA31* gene, which was found in four isolates retrieved from animals in three different batches that were present at the same time in the farm for several weeks (Figure 4(B)). Variation in the ARGs within an ICE can be expected given recombination and IS-mediated integration events (Beker et al. 2018), and in fact the composition found here in ICE Tn7407-like resembles the findings described by Cameron et al. who found variations in the syntenous resistance region 2 of ICE*Mh1*, an ICE related to ICE*Pmu1* (Eidam et al. 2015), with the addition of *aadA31*. From an

evolutionary perspective, these recombination events suggest ICE Tn7407, first detected in animals in batch LV1 from feedlot 1 (isolates 166CV and 189CV) was experiencing microevolution through the gain of *aadA31* (found in isolates carrying ICE Tn7407-like from animals in batches LV4, LV8 and LV9) (Figure 4(B)). According to our analysis the same ICE (Tn7407 plus the addition of *aadA31*) was present in three US isolates retrieved nine years before the Tn7407 was formally described (Supplementary Table S2), further demonstrating the risk of acquisition of new ARGs by these mobile structures. The cluster of closely related seven isolates from subclade 3.2 carried two ICEs in separate parts of their genomes, in what is to the best of our knowledge the first instance of such occurrence in the *P. multocida*. Detection and characterization of new ICEs linked to MDR phenotypes in *P. multocida* is important in order to evaluate the usefulness of newly developed PCR techniques aiming at the direct detection of already described ICEs as indication of the presence of MDR-BRD pathogens (Conrad et al. 2024).

Interestingly, isolates from subclade 3.1, despite sharing several resistance genes with those from subclade 3.2 such as *aph(3'')-Ib*, *aph(6)-Id*, *mefC*, *mphG*, *sul2*, and *tet(Y)*, did not carry them on ICEs but on a prophage and an element flanked by two copies of IS*Mha6* (putative composite transposon). Although the presence of prophages in *P. multocida* has been demonstrated in several studies, they have been mostly associated with the carriage of function-unknown proteins and not with antibiotic-resistance genes (Yu et al. 2016; Hurtado et al. 2020). Similarly, reports describing composite transposons are very rare, with the first identified in *P. multocida* being Tn5706, a transposon of about 4kb associated with tetracycline resistance gene *tet(H)* (Kehrenberg et al. 1998). In that case, Tn5706 was flanked by IS1592 (from the IS982 family), whereas in our case, the putative composite transposon was flanked by IS*Mha6* (from the IS1595 family). These results demonstrate that other mobile genetic elements may be also involved in the dissemination of ARGs in BRD bacterial pathogens, and these could be missed in studies in which detection is based exclusively on PCRs aiming only at ICE's associated genes.

The recent increase in AMR and MDR of BRD bacterial pathogens isolated from animals in feedlots has been linked to the use of metaphylaxis with macrolides at arrival processing (Snyder et al. 2017; Timsit et al. 2017; Guo et al. 2020; Andrés-Lasheras et al. 2021; Hirsch et al. 2022). Since resistance in *P. multocida* is mainly associated with the presence of ICEs that contain genes conferring resistance to multiple antimicrobials (Michael et al. 2018; Snyder and Credille 2020; Andrés-Lasheras et al. 2022), this practice can favor the persistence and dissemination of resistant strains. In this study, different mobile genetic elements, including ICEs, a prophage and a putative composite transposon, associated with ARGs linked to phenotypic MDR profiles have been found in isolates from feedlot cattle housed in different batches in several feedlots in

Spain. These results point out the complexity of AMR genotypic mechanisms in *P. multocida*, demonstrate the risk of selecting MDR strains when single antimicrobial-based treatments are used in cattle upon arrival at feedlots, and underline the need for implementing antimicrobial surveillance programs to control and reduce the spread of antimicrobial resistance in these pathogens within and between herds.

Disclosure statement

No potential conflict of interest was reported by the author(s).

Funding

PID2021-125136OB-I00 (AMR-EPIPLAS) funded by MCIN/AEI and ERDF – a way of making Europe. This study was supported by Ministry of Science, Technology and Innovation of Colombia.

Data availability statement

The genomic data generated in this research have been deposited in ENA under project PRJNA988320.

References

- Alhamami T, Roy Chowdhury P, Venter H, Veltman T, Truswell A, Abraham S, Sapula SA, Carr M, Djordjevic SP, Trott DJ. 2023. Genomic profiling of *Pasteurella multocida* isolated from feedlot cases of bovine respiratory disease. *Vet Microbiol.* 283:109773. doi:10.1016/j.vetmic.2023.109773.
- Andrés-Lasheras S, Ha R, Zaheer R, Lee C, Booker CW, Dorin C, Van Donkersgoed J, Deardon R, Gow S, Hannon SJ, et al. 2021. Prevalence and risk factors associated with antimicrobial resistance in bacteria related to bovine respiratory disease – a broad cross-sectional study of beef cattle at entry into Canadian feedlots. *Front Vet Sci.* 8:692646. doi:10.3389/fvets.2021.692646.
- Andrés-Lasheras S, Jelinski M, Zaheer R, McAllister TA. 2022. Bovine respiratory disease: conventional to culture-independent approaches to studying antimicrobial resistance in North America. *Antibiotics (Basel).* 11(4):487. doi:10.3390/antibiotics11040487.
- Andrews S. 2010. FastQC: a quality control tool for high throughput sequence data [Computer software]. <http://www.bioinformatics.babraham.ac.uk/projects/fastqc>.
- Anholt RM, Klima C, Allan N, Matheson-Bird H, Schatz C, Ajitkumar P, Otto SJ, Peters D, Schmid K, Olson M, et al. 2017. Antimicrobial susceptibility of bacteria that cause bovine respiratory disease complex in Alberta, Canada. *Front Vet Sci.* 4:207. doi:10.3389/fvets.2017.00207.
- Bankevich A, Nurk S, Antipov D, Gurevich AA, Dvorkin M, Kulikov AS, Lesin VM, Nikolenko SI, Pham S, Prijbelski AD, et al. 2012. SPAdes: a new genome assembly algorithm and its applications to single-cell sequencing. *J Comput Biol.* 19(5):455–477. doi:10.1089/cmb.2012.0021.
- Becker J, Perreten V, Schüpbach-Regula G, Stucki D, Steiner A, Meylan M. 2022. Associations of antimicrobial use with antimicrobial susceptibility at the calf level in bacteria isolated from the respiratory and digestive tracts of veal calves before slaughter. *J Antimicrob Chemother.* 77(10):2859–2866. doi:10.1093/jac/dkac246.
- Beker M, Rose S, Lykkebo CA, Douthwaite S. 2018. Integrative and conjugative elements (ICEs) in *Pasteurellaceae* species and their detection by multiplex PCR. *Front Microbiol.* 9:1329. doi:10.3389/fmicb.2018.01329.
- Bolger AM, Lohse M, Usadel B. 2014. Trimmomatic: a flexible trimmer for Illumina sequence data. *Bioinformatics.* 30(15):2114–2120. doi:10.1093/bioinformatics/btu170.
- Calderón Bernal JM, Fernández A, Arnal JL, Sanz Tejero C, Fernández-Garayzábal JF, Vela AI, Cid D. 2022. Molecular epidemiology of *Pasteurella multocida* associated with bovine respiratory disease outbreaks. *Animals (Basel).* 13(1):75. doi:10.3390/ani13010075.
- Calderón Bernal JM, Serna C, García Muñoz Á, Díez Guerrier A, Domínguez L, Fernández-Garayzábal JF, Vela AI, Cid D. 2023. Genotypic comparison of *Pasteurella multocida* from healthy animals at entry to the feedlots with that and from bovine respiratory disease-affected animals during the fattening period. *Animals (Basel).* 13(17):2687. doi:10.3390/ani13172687.
- Cameron A, Klima CL, Ha R, Gruninger RJ, Zaheer R, McAllister TA. 2018. A novel aadA aminoglycoside resistance Gene in bovine and porcine pathogens. *mSphere.* 3(1):e00568–17. doi:10.1128/mSphere.00568-17.
- Carattoli A, Zankari E, García-Fernández A, Voldby Larsen M, Lund O, Villa L, Møller Aarestrup F, Hasman H. 2014. *In silico* detection and typing of plasmids using PlasmidFinder and plasmid multilocus sequence typing. *Antimicrob Agents Chemother.* 58(7):3895–3903. doi:10.1128/AAC.02412-14.
- Catry B, Dewulf J, Maes D, Pardon B, Callens B, Vanrobaeys M, Opsomer G, Kruif A. d, Haesebrouck F. 2016. Effect of antimicrobial consumption and production type on antibacterial resistance in the bovine respiratory and digestive tract. *PLoS One.* 11(1):e0146488. doi:10.1371/journal.pone.0146488.
- Chen S-Y, Negri Bernardino P, Fausak E, Van Noord M, Maier G. 2022. Scoping review on risk factors and methods for the prevention of bovine respiratory disease applicable to cow-calf operations. *Animals (Basel).* 12(3):334. doi:10.3390/ani12030334.
- Cheng L, Connor TR, Sirén J, Aanensen DM, Corander J. 2013. Hierarchical and spatially explicit clustering of DNA sequences with BAPS software. *Mol Biol Evol.* 30(5):1224–1228. doi:10.1093/MOLBEV/MST028.
- Clawson ML, Murray RW, Sweeney MT, Apley MD, DeDonder KD, Capik SF, Larson RL, Lubbers BV, White BJ, Kalbfleisch TS, et al. 2016. Genomic signatures of *Mannheimia haemolytica* that associate with the lungs of cattle with respiratory disease, an integrative conjugative element, and antibiotic resistance genes. *BMC Genomics.* 17(1):982. doi:10.1186/s12864-016-3316-8.
- Clinical and Laboratory Standards Institute (CLSI). 2008. Performance standards for antimicrobial disk and dilution susceptibility tests for bacteria isolated from animals: approved Standard. 4th ed. Wayne, PA: Clinical and Laboratory Standard Institute.
- Conrad CC, Funk T, Andrés-Lasheras S, Yevtushenko C, Claassen C, Otto SJG, Waldner C, Zaheer R, McAllister TA. 2024. Improving the detection of integrative conjugative elements in bovine nasopharyngeal swabs using multiplex recombinase polymerase amplification. *J Microbiol Methods.* 221:106943. doi:10.1016/j.mimet.2024.106943.
- Corander J, Marttinen P. 2006. Bayesian identification of admixture events using multilocus molecular markers. *Mol Ecol.* 15(10):2833–2843. doi:10.1111/J.1365-294X.2006.02994.X.
- Corander J, Waldmann P, Marttinen P, Sillanpää MJ. 2004. BAPS 2: enhanced possibilities for the analysis of genet-

- ic population structure. *Bioinformatics*. 20(15):2363–2369. doi:[10.1093/BIOINFORMATICS/BTH250](https://doi.org/10.1093/BIOINFORMATICS/BTH250).
- Corander J, Waldmann P, Sillanpää MJ. 2003. Bayesian analysis of genetic differentiation between populations. *Genetics*. 163(1):367–374. doi:[10.1093/GENETICS/163.1.367](https://doi.org/10.1093/GENETICS/163.1.367).
- Crosby WB, Karisch BB, Hiott LM, Pinnell LJ, Pittman A, Frye JG, Jackson CR, Loy JD, Epperson WB, Blanton J, et al. 2023. Tulathromycin metaphylaxis increases nasopharyngeal isolation of multidrug resistant *Mannheimia haemolytica* in stocker heifers. *Front Vet Sci*. 10:1256997. doi:[10.3389/fvets.2023.1256997](https://doi.org/10.3389/fvets.2023.1256997).
- Croucher NJ, Page AJ, Connor TR, Delaney AJ, Keane JA, Bentley SD, Parkhill J, Harris SR. 2015. Rapid phylogenetic analysis of large samples of recombinant bacterial whole genome sequences using Gubbins. *Nucleic Acids Res*. 43(3):e15–e15. doi:[10.1093/nar/gku1196](https://doi.org/10.1093/nar/gku1196).
- Cury J, Abby SS, Doppelt-Azeroual O, Néron B, Rocha EPC. 2020. Identifying conjugative plasmids and integrative conjugative elements with CONJscan. *Methods Mol Biol*. 2075:265–283. doi:[10.1007/978-1-4939-9877-7_19](https://doi.org/10.1007/978-1-4939-9877-7_19).
- Darling ACE, Mau B, Blattner FR, Perna NT. 2004. Mauve: multiple alignment of conserved genomic sequence with rearrangements. *Genome Res*. 14(7):1394–1403. doi:[10.1101/gr.2289704](https://doi.org/10.1101/gr.2289704).
- De Coster W, D'Hert S, Schultz DT, Cruts M, Van Broeckhoven C. 2018. NanoPack: visualizing and processing long-read sequencing data. *Bioinformatics*. 34(15):2666–2669. doi:[10.1093/bioinformatics/bty149](https://doi.org/10.1093/bioinformatics/bty149).
- de Jong A, Morrissey I, Rose M, Temmerman R, Klein U, Simjee S, El Garch F. 2023. Antimicrobial susceptibility among respiratory tract pathogens isolated from diseased cattle and pigs from different parts of Europe. *J Appl Microbiol*. 134(8):lxad132. doi:[10.1093/jambio/lxad132](https://doi.org/10.1093/jambio/lxad132).
- DeDonder KD, Apley MD. 2015. A literature review of antimicrobial resistance in Pathogens associated with bovine respiratory disease. *Anim Health Res Rev*. 16(2):125–134. doi:[10.1017/S146625231500016X](https://doi.org/10.1017/S146625231500016X).
- Eidam C, Poehlein A, Leimbach A, Michael GB, Kadlec K, Liesegang H, Daniel R, Sweeney MT, Murray RW, Watts JL, et al. 2015. Analysis and comparative genomics of ICEMh1, a novel integrative and conjugative element (ICE) of *Mannheimia haemolytica*. *J Antimicrob Chemother*. 70(1):93–97. doi:[10.1093/jac/dku361](https://doi.org/10.1093/jac/dku361).
- Feldgarden M, Brover V, Gonzalez-Escalona N, Frye JG, Haendiges J, Haft DH, Hoffmann M, Pettengill JB, Prasad AB, Tillman GE, et al. 2021. AMRFinderPlus and the Reference Gene Catalog facilitate examination of the genomic links among antimicrobial resistance, stress response, and virulence. *Sci Rep*. 11(1):12728. doi:[10.1038/s41598-021-91456-0](https://doi.org/10.1038/s41598-021-91456-0).
- Guo Y, McMullen C, Timsit E, Hallewell J, Orsel K, van der Meer F, Yan S, Alexander TW. 2020. Genetic relatedness and antimicrobial resistance in respiratory bacteria from beef calves sampled from spring processing to 40 days after feedlot entry. *Vet Microbiol*. 240:108478. doi:[10.1016/j.vetmic.2019.108478](https://doi.org/10.1016/j.vetmic.2019.108478).
- Gurevich A, Saveliev V, Vyahhi N, Tesler G. 2013. QUAST: quality assessment tool for genome assemblies. *Bioinformatics*. 29(8):1072–1075. doi:[10.1093/bioinformatics/btt086](https://doi.org/10.1093/bioinformatics/btt086).
- Hirsch C, Timsit E, Uddin MS, Guan LL, Alexander TW. 2022. Comparison of pathogenic bacteria in the upper and lower respiratory tracts of cattle either directly transported to a feedlot or co-mingled at auction markets prior to feedlot placement. *Front Vet Sci*. 9:1026470. doi:[10.3389/fvets.2022.1026470](https://doi.org/10.3389/fvets.2022.1026470).
- Hurtado R, Maturrano L, Azevedo V, Aburjaile F. 2020. Pathogenomics insights for understanding *Pasteurella multocida* adaptation. *Int J Med Microbiol*. 310(4):151417. doi:[10.1016/j.ijmm.2020.151417](https://doi.org/10.1016/j.ijmm.2020.151417).
- Jobman E, Hagenmaier J, Meyer N, Harper LB, Taylor L, Lukasiewicz K, Thomson D, Lowe J, Terrell S. 2023. Cross-section observational study to assess antimicrobial resistance prevalence among bovine respiratory disease bacterial isolates from commercial US feedlots. *Antibiotics (Basel)*. 12(2):215. doi:[10.3390/antibiotics12020215](https://doi.org/10.3390/antibiotics12020215).
- Kehrenberg C, Schwarz S. 2007. Mutations in 16S rRNA and ribosomal protein S5 associated with high-level spectinomycin resistance in *Pasteurella multocida*. *Antimicrob Agents Chemother*. 51(6):2244–2246. doi:[10.1128/AAC.00229-07](https://doi.org/10.1128/AAC.00229-07).
- Kehrenberg C, Werckenthin C, Schwarz S. 1998. Tn5706, a transposon-like element from *Pasteurella multocida* mediating tetracycline resistance. *Antimicrob Agents Chemother*. 42(8):2116–2118. doi:[10.1128/AAC.42.8.2116](https://doi.org/10.1128/AAC.42.8.2116).
- Klima CL, Cook SR, Zaheer R, Laing C, Gannon VP, Xu Y, Rasmussen J, Potter A, Hendrick S, Alexander TW, et al. 2016. Comparative genomic analysis of *Mannheimia haemolytica* from bovine sources. *PLoS One*. 11(2):e0149520. doi:[10.1371/journal.pone.0149520](https://doi.org/10.1371/journal.pone.0149520).
- Klima CL, Holman DB, Cook SR, Conrad CC, Ralston BJ, Allan N, Anholt RM, Niu YD, Stanford K, Hannon SJ, et al. 2020. Multidrug resistance in Pasteurellaceae associated with bovine respiratory disease mortalities in North America from 2011 to 2016. *Front Microbiol*. 11:638008. doi:[10.3389/fmicb.2020.606438](https://doi.org/10.3389/fmicb.2020.606438).
- Klima CL, Zaheer R, Cook SR, Booker CW, Hendrick S, Alexander TW, McAllister TA. 2014. Pathogens of bovine respiratory disease in North American feedlots conferring multidrug resistance via integrative conjugative elements. *J Clin Microbiol*. 52(2):438–448. doi:[10.1128/jcm.02485-13](https://doi.org/10.1128/jcm.02485-13).
- Kong L-C, Gao D, Gao Y-H, Liu S-M, Ma H-X. 2014. Fluoroquinolone resistance mechanism of clinical isolates and selected mutants of *Pasteurella multocida* from bovine respiratory disease in China. *J Vet Med Sci*. 76(12):1655–1657. doi:[10.1292/jvms.14-0240](https://doi.org/10.1292/jvms.14-0240).
- Kostova V, Hanke D, Kaspar H, Fiedler S, Schwarz S, Krüger-Haker H. 2024. Macrolide resistance in *Mannheimia haemolytica* isolates associated with bovine respiratory disease from the German national resistance monitoring program GERM-Vet 2009 to 2020. *Front Microbiol*. 15:1356208. doi:[10.3389/fmicb.2024.1356208](https://doi.org/10.3389/fmicb.2024.1356208).
- Kudirkiene E, Aagaard AK, Schmidt LMB, Pansri P, Krogh KM, Olsen JE. 2021. Occurrence of major and minor pathogens in calves diagnosed with bovine respiratory disease. *Vet Microbiol*. 259:109135. doi:[10.1016/j.vetmic.2021.109135](https://doi.org/10.1016/j.vetmic.2021.109135).
- Letunic I, Bork P. 2019. Interactive Tree Of Life (iTOL) v4: recent updates and new developments. *Nucleic Acids Res*. 47(W1):W256–W259. doi:[10.1093/nar/gkz239](https://doi.org/10.1093/nar/gkz239).
- Maples WE, Brorsen BW, Peel D, Hicks B. 2022. Observational study of the effect of metaphylaxis treatment on feedlot cattle productivity and health. *Front Vet Sci*. 9:947585. doi:[10.3389/fvets.2022.947585](https://doi.org/10.3389/fvets.2022.947585).
- Marçais G, Delcher AL, Phillippy AM, Coston R, Salzberg SL, Zimin A. 2018. MUMmer4: a fast and versatile genome alignment system. *PLoS Comput Biol*. 14(1):e1005944. doi:[10.1371/journal.pcbi.1005944](https://doi.org/10.1371/journal.pcbi.1005944).
- Melchner A, van de Berg S, Scuda N, Feuerstein A, Hanczaruk M, Schumacher M, Straubinger RK, Marosevic D, Riehm JM. 2021. Antimicrobial resistance in isolates from cattle with bovine respiratory disease in Bavaria, Germany. *Antibiotics (Basel)*. 10(12):1538. doi:[10.3390/antibiotics10121538](https://doi.org/10.3390/antibiotics10121538).

- Michael GB, Bossé JT, Schwarz S. 2018. Antimicrobial resistance in Pasteurellaceae of veterinary origin. *Microbiol Spectr.* 6(3):10.1128. doi:10.1128/microbiolspec.ARBA-0022-2017.
- Michael GB, Kadlec K, Sweeney MT, Brzuszkiewicz E, Liesegang H, Daniel R, Murray RW, Watts JL, Schwarz S. 2012a. ICEPmu1, an integrative conjugative element (ICE) of *Pasteurella multocida*: analysis of the regions that comprise 12 antimicrobial resistance genes. *J Antimicrob Chemother.* 67(1):84–90. doi:10.1093/jac/dkr406.
- Michael GB, Kadlec K, Sweeney MT, Brzuszkiewicz E, Liesegang H, Daniel R, Murray RW, Watts JL, Schwarz S. 2012b. ICEPmu1, an integrative conjugative element (ICE) of *Pasteurella multocida*: structure and transfer. *J Antimicrob Chemother.* 67(1):91–100. doi:10.1093/jac/dkr411.
- Néron B, Denise R, Coluzzi C, Touchon M, Rocha EPC, Abby SS. 2023. MacSyFinder v2: improved modelling and search engine to identify molecular systems in genomes. *Peer Community J.* 3, article no. e28. doi:10.24072/pc-journal.250.
- Nielsen SS, Bicoût DJ, Calistri P, Canali E, Drewe JA, Garin-Bastuji B, Gonzales Rojas JL, Gortazar Schmidt C, Herskin M, Michel V, EFSA Panel on Animal Health and Welfare (AHAW), et al. 2021. Assessment of animal diseases caused by bacteria resistant to antimicrobials: cattle. *EFSA J.* 19(12):e06955. doi:10.2903/j.efsa.2021.6955.
- Nobrega D, Andres-Lasheras S, Zaheer R, McAllister T, Homerosky E, Anholt RM, Dorin C. 2021. Prevalence, risk factors, and antimicrobial resistance profile of respiratory pathogens isolated from suckling beef calves to reprocessing at the feedlot: a longitudinal study. *Front Vet Sci.* 8:764701. doi:10.3389/fvets.2021.764701.
- Olsen AS, Warrass R, Douthwaite S. 2015. Macrolide resistance conferred by rRNA mutations in field isolates of *Mannheimia haemolytica* and *Pasteurella multocida*. *J Antimicrob Chemother.* 70(2):420–423. doi:10.1093/jac/dku385.
- Owen JR, Noyes N, Young AE, Prince DJ, Blanchard PC, Lehenbauer TW, Aly SS, Davis JH, O'Rourke SM, Abdo Z, et al. 2017. Whole-genome sequencing and concordance between antimicrobial susceptibility genotypes and phenotypes of bacterial isolates associated with bovine respiratory disease. G3 (Bethesda). 7(9):3059–3071. doi:10.1534/g3.117.1137.
- Page AJ, Taylor B, Delaney AJ, Soares J, Seemann T, Keane JA, Harris SR. 2016. SNP-sites: rapid efficient extraction of SNPs from multi-FASTA alignments. *Microb Genom.* 2(4):e000056. doi:10.1099/mgen.0.000056.
- R Core Team. 2021. R: a language and environment for statistical computing [Computer software]. Vienna: R Foundation for Statistical Computing. <https://www.R-project.org/>.
- Robertson J, Nash JHE. 2018. MOB-suite: software tools for clustering, reconstruction and typing of plasmids from draft assemblies. *Microb Genom.* 4(8):e000206. doi:10.1099/mgen.0.000206.
- Roy Chowdhury P, Alhamami T, Venter H, Veltman T, Carr M, Mollinger J, Trott DJ, Djordjevic SP. 2024. Identification and evolution of ICE-PmuST394: a novel integrative conjugative element in *Pasteurella multocida* ST394. *J Antimicrob Chemother.* 79(4):851–858. doi:10.1093/jac/dkac040.
- Schink AK, Hanke D, Semmler T, Brombach J, Bethe A, Lübke-Becker A, Teske K, Müller KE, Schwarz S. 2022. Novel multiresistance-mediating integrative and conjugative elements carrying unusual antimicrobial resistance genes in *Mannheimia haemolytica* and *Pasteurella multocida*. *J Antimicrob Chemother.* 77(7):2033–2035. doi:10.1093/jac/dkac116.
- Schönecker L, Schnyder P, Schüpbach-Regula G, Meylan M, Overesch G. 2020. Prevalence and antimicrobial resistance of opportunistic pathogens associated with bovine respiratory disease isolated from nasopharyngeal swabs of veal calves in Switzerland. *Prev Vet Med.* 185:105182. doi:10.1016/j.prevetmed.2020.105182.
- Schwengers O, Jelonek L, Dieckmann MA, Beyvers S, Blom J, Goesmann A. 2021. Bakta: rapid and standardized annotation of bacterial genomes via alignment-free sequence identification. *Microb Genom.* 7(11):000685. doi:10.1099/mgen.0.000685.
- Smith RA, Step DL, Woolums AR. 2020. Bovine respiratory disease: looking back and looking forward, what do we see? *Vet Clin North Am Food Anim Pract.* 36(2):239–251. doi:10.1016/j.cvfa.2020.03.009.
- Snyder E, Credille B, Berghaus R, Giguère S. 2017. Prevalence of multi drug antimicrobial resistance in isolated from high-risk stocker cattle at arrival and two weeks after processing. *J Anim Sci.* 95(3):1124–1131. doi:10.2527/jas.2016.1110.
- Snyder E, Credille B. 2020. *Mannheimia haemolytica* and *Pasteurella multocida* in bovine respiratory disease. *Veterinary Clinics of North America: food Animal Practice.* 36(2):253–268. doi:10.1016/j.cvfa.2020.02.001.
- Stamatakis A. 2014. RAxML version 8: a tool for phylogenetic analysis and post-analysis of large phylogenies. *Bioinformatics.* 30(9):1312–1313. doi:10.1093/bioinformatics/btu033.
- Stanford K, Zaheer R, Klima C, McAllister T, Peters D, Niu YD, Ralston B. 2020. Antimicrobial resistance in members of the bacterial bovine respiratory disease complex isolated from lung tissue of cattle mortalities managed with or without the use of antimicrobials. *Microorganisms.* 8(2):288. doi:10.3390/microorganisms8020288.
- Timsit E, Hallewell J, Booker C, Tison N, Amat S, Alexander TW. 2017. Prevalence and antimicrobial susceptibility of *Mannheimia haemolytica*, *Pasteurella multocida*, and *Histophilus somni* isolated from the lower respiratory tract of healthy feedlot cattle and those diagnosed with bovine respiratory disease. *Vet Microbiol.* 208:118–125. doi:10.1016/j.vetmic.2017.07.013.
- Tonkin-Hill G, Lees JA, Bentley SD, Frost SDW, Corander J. 2018. RhierBAPS: an R implementation of the population clustering algorithm hierBAPS. *Wellcome Open Res.* 3:93. doi:10.12688/wellcomeopenres.14694.1.
- Tonkin-Hill G, Lees JA, Bentley SD, Frost SDW, Corander J. 2019. Fast hierarchical Bayesian analysis of population structure. *Nucleic Acids Res.* 47(11):5539–5549. doi:10.1093/nar/gkz361.
- Ujvári B, Magyar T. 2022. Investigation of macrolide resistance genotypes of *Pasteurella multocida* isolates from cattle and small ruminants. *Microb Drug Resist.* 28(9):941–947. doi:10.1089/mdr.2022.0010.
- Wick RR, Judd LM, Gorrie CL, Holt KE. 2017. Unicycler: resolving bacterial genome assemblies from short and long sequencing reads. *PLoS Comput Biol.* 13(6):e1005595. doi:10.1371/journal.pcbi.1005595.
- Wick RR, Schultz MB, Zobel J, Holt KE. 2015. Bandage: interactive visualization of *de novo* genome assemblies. *Bioinformatics.* 31(20):3350–3352. doi:10.1093/bioinformatics/btv383.
- Wishart DS, Han S, Saha S, Oler E, Peters H, Grant JR, Stothard P, Gautam V. 2023. PHASTEST: faster than PHASTER, better than PHAST. *Nucleic Acids Res.* 51(W1):W443–W450. doi:10.1093/nar/gkad382.
- Woolums AR, Karisch BB, Frye JG, Epperson W, Smith DR, Blanton J, Austin F, Kaplan R, Hiott L, Woodley T, et al.

2018. Multidrug resistant *Mannheimia haemolytica* isolated from high-risk beef stocker cattle after antimicrobial metaphylaxis and treatment for bovine respiratory disease. Vet Microbiol. 221:143–152. doi:[10.1016/j.vet-mic.2018.06.005](https://doi.org/10.1016/j.vet-mic.2018.06.005).

Yu C, Sizhu S, Luo Q, Xu X, Fu L, Zhang A. 2016. Genome sequencing of a virulent avian *Pasteurella multocida* strain GX-Pm reveals the candidate genes involved in the pathogenesis. Res Vet Sci. 105:23–27. doi:[10.1016/j.rvsc.2016.01.013](https://doi.org/10.1016/j.rvsc.2016.01.013).